

Non-monotonic emergence of order from chaos in acoustically-coupled turbulent thermo-fluid systems

Aswin Balaji,^{1,2} Shruti Tandon,^{1,2} Norbert Marwan,^{3,4} Jürgen Kurths,^{3,5}
R. I. Sujith^{1,2*}

¹Department of Aerospace Engineering, Indian Institute of Technology Madras, Chennai 600036, India

²Centre of Excellence for studying Critical Transitions in Complex Systems

Indian Institute of Technology Madras, Chennai 600036, India

³Potsdam Institute for Climate Impact Research (PIK)

Potsdam 14473, Germany

⁴Institute of Geosciences, University of Potsdam, Potsdam 14476, Germany

⁵Institute of Physics, Humboldt Universität zu Berlin, Berlin 12489, Germany

*Corresponding author: sujith@iitm.ac.in

Self-sustained order can emerge in complex systems due to internal feedback between coupled subsystems. Although the general mechanisms are known, the specific paths of transition to order can be different in distinct systems. Here, we present our discovery of a surprisingly non-monotonic emergence of order amidst chaos in a turbulent thermo-acoustic fluid system. Fluctuations play a vital role in determining the dynamical state and transitions in a system, as theorized by Prigogine. In this work, we use the framework of complex networks and encode the amplitude scales of fluctuations in the topology of a network. Using network entropy, we identify the amount of uncertainty in fluctuations and use it as a measure of chaotic intensity. Further, we show

that network centrality measures capture the magnitude jumps in amplitude scales due to fluctuations. We find that the competition between turbulence and nonlinear interactions leads to the non-monotonic emergence of order amidst chaos in turbulent thermo-acoustic fluid systems.

Short title: Non-monotonic emergence of order from chaos

Teaser: Emergence of order in acoustically-coupled turbulent thermo-fluid system is non-monotonous; disorder increases and then decreases.

INTRODUCTION

Diverse systems exhibit the emergence of ordered dynamics from disorder. Fireflies flashing in synchrony (1), rhythmic applause of audience (2), synchronous discharge of neurons causing epileptic seizures (3), oscillatory chemical reactions in Belousov–Zhabotinsky reaction (4), spatio-temporal patterns in surface chemical soup (5), biochemical oscillators such as glycolytic oscillators (6), pattern formation in fluid motion during convective instabilities (7), and the emergence of a single coherent electromagnetic wave in lasers (8) are some typical examples of order emerging from disorder. Furthermore, the emergence of order in the form of oscillatory dynamics has been reported in turbulent thermo-fluid systems (9–13), and aerodynamic fluttering of slender structures such as bridges and wings of an aircraft (14, 15).

The emergence of ordered dynamics in such diverse systems is a consequence of self-organization and nonlinear interactions amongst the sub-units of the system (16, 17). Additionally, the spatio-temporal structure of interactions, the functional behavior of sub-units, and the fluctuations in system variables are interdependent (18). Fluctuations are inherently present in systems and are damped out for certain control parameter values. With a change in the control parameter, these fluctuations may amplify and aid in the selection of a new ordered dynamical

state. Ordered dynamics, such as periodic oscillations, can be viewed as a giant macroscopic fluctuation in itself.

The emergence of order through fluctuations, as first discussed by Prigogine (18), is an intriguing phenomenon and raises interesting questions about the occurrence of fluctuations. For example, what are the characteristic features of fluctuations during distinct dynamical states? How do these fluctuations evolve during the emergence of order? And, can we relate the variations in the amplitude scales of fluctuations to the dynamical transitions in the system? In this study, we analyze the variation in fluctuations during the transition from chaos to order in the temporal dynamics of a complex thermo-fluid system.

We study an experimental turbulent thermoacoustic system where the acoustic field, the underlying turbulent flow, and the combustion dynamics are interdependent (19–21). Thermoacoustic systems find applications in gas turbine combustors and rocket engines (20). In such combustion systems, the control parameter is the flow rate of the inlet fuel-air mixture, quantified by the Reynolds number (Re) (see Materials and Methods section for details). Fuel is injected into an airflow of high Reynolds number (turbulent conditions) and undergoes combustion in a closed duct.

Inside a closed duct, as the Reynolds number of the inlet flow increases, the turbulence intensity increases as well (22). Turbulence introduces a wide range of time and length scales (23), thus promoting chaotic dynamics. Also, flow in a confinement creates an acoustic field. Heat released due to the combustion of the fuel-air mixture adds energy to the fluctuations in the acoustic field. Perturbations in the acoustic field influence the flame surface oscillations, leading to fluctuations in the heat release rate. Further, the acoustic and hydrodynamic fluctuations together influence the mixing and convection of the fuel-air mixture via coherent structures in the flow, which subsequently determine the dynamics of the turbulent thermo-fluid system.

In summary, fluctuations in one subsystem depend on the function of other subsystems and

the spatio-temporal structure of the inter-subsystem interactions (21). While turbulence promotes disorder and chaos, nonlinear feedback between subsystems promotes self-organization. Although the range of spatial and temporal scales increases with Re , we observe the emergence of a single dominant frequency in acoustic pressure, periodic shedding of large coherent structures, and sudden and intense heat release patterns occurring periodically (24). In this work, we investigate the variations in the fluctuations in the acoustic pressure field of the combustor with changes in the control parameter of the system. Studying the acoustic field, we decipher the interplay between turbulence and nonlinear feedback on the dynamics of the system.

Turbulent thermoacoustic systems are known to exhibit a transition from low-amplitude chaos (25) (Fig. 1D) to high-amplitude periodic oscillations (order) (refer Fig. 1F) in the acoustic field with an increase in the Reynolds number (Re) of the inlet flow (13, 20). Such a transition occurs via the route of intermittency (26), which is characterized by bursts of high-amplitude periodic oscillations amidst epochs of low-amplitude chaotic oscillations in the acoustic field (Fig. 1E). The ordered dynamics obtained at high Re is a high-amplitude limit cycle oscillation, termed as thermoacoustic instability, which can cause a catastrophic destruction to engines and restrict their operational envelope (13, 20).

Self-sustained periodic dynamics during thermoacoustic instability has also been viewed as synchronization between two coupled non-identical oscillators representing the heat release rate and acoustic pressure fluctuations (27). Further, complex networks have been used to analyze the characteristics of temporal dynamics (28–35) during the transition from chaos to order in such systems. The presence of scale-invariant fluctuations during chaotic dynamics and the loss of such scale-invariance during the emergence of order was discovered by means of visibility graphs (29). Further, complex networks built from the phase space cycles delineated the transformation in the topology of the phase space from a set of several unstable periodic orbits to a single stable limit cycle orbit as the system dynamics transition from chaos to order via

intermittency (35).

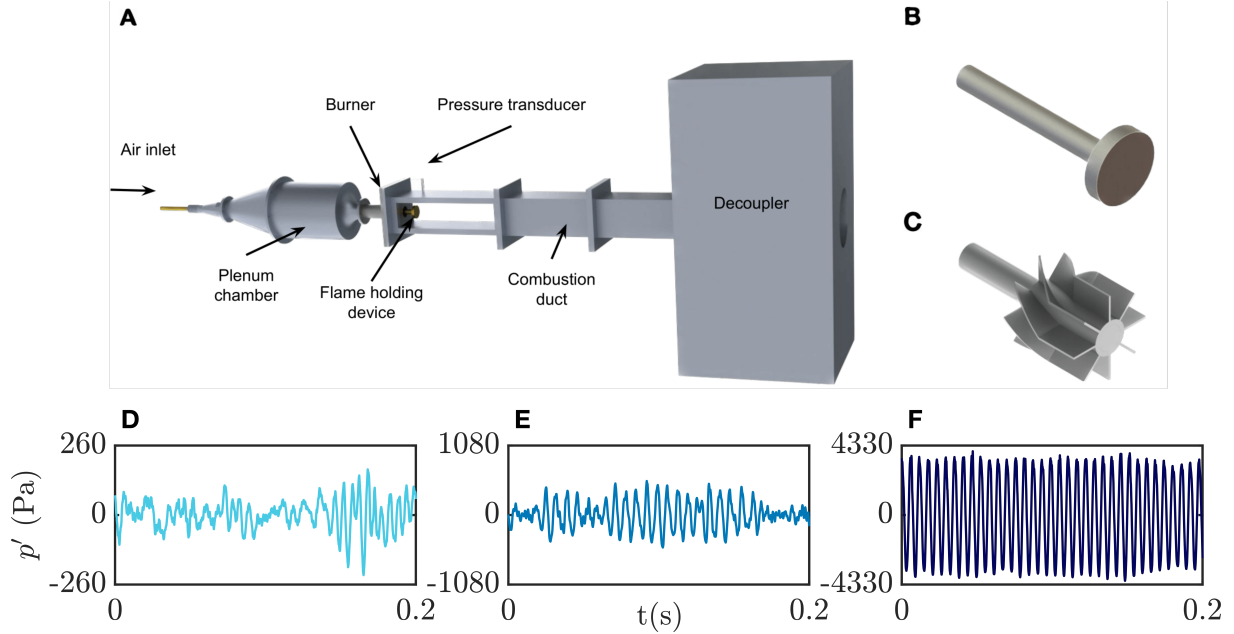


Figure 1: **Experimental setup and time series of acoustic pressure fluctuations corresponding to different dynamical states.** (A) Schematic of the turbulent combustor used in this study. Air at room temperature enters the plenum chamber through the inlet and gets mixed with the fuel before entering the combustion chamber, where combustion occurs. The flame holding device in the combustion duct is essential to maintain sustained combustion. The flame holding devices that were used to perform experiments are - (B) circular bluff-body and (C) vane swirler. The time series of acoustic pressure variation in a bluff-body stabilized turbulent combustor during the state of (D) low-amplitude aperiodic fluctuations (chaos) ($Re = 3.865 \times 10^4$) (E) intermittency ($Re = 5.083 \times 10^4$) (F) thermoacoustic instability (order) ($Re = 6.759 \times 10^4$).

Here, we use complex networks to encode the fluctuations in the temporal dynamics of the acoustic pressure fluctuations (p'). A network is derived from the experimental time series of p' where the amplitude bins are the nodes, and the weight of a link between two nodes defines the probability of transition between the respective amplitude bins (36, 37). We refer to the resulting network as amplitude transition network. The amount of disorder in the dynamics, referred here as the chaotic intensity, is encoded in the network via the transition probabilities due to fluctuations in a system variable. We introduce the use of the mean Shannon entropy

of an amplitude transition network to quantify the chaotic intensity during different dynamical states. Further, we use distance-based centrality measures derived from the network to capture the diversity in the magnitude of amplitude jumps owing to fluctuations.

In our system, we find that the amount of disorder varies non-monotonically with the Reynolds number of the inlet flow. It is worth noting that in certain systems, order can emerge in a monotonic manner either gradually (38,39) or abruptly (40). However, in our complex thermo-fluid system, we discover that the chaotic intensity initially increases and then decreases as the system transitions to ordered dynamics. Moreover, we find a scaling law relation between the network measures and the root-mean-square of the acoustic pressure fluctuations during both increase and decrease of chaotic content in the system.

RESULTS

Prigogine (18) theorized that macroscopic order occurs in a system owing to the interplay between the function of the sub-units, spatio-temporal structure of interactions, and the fluctuations in the system variables. The structure, function, and fluctuations in a system are interdependent, and a variation in either of them reflects the changes in the state of the system. In order to decipher the dynamical evolution of an acoustically-coupled turbulent thermo-fluid system, we characterize the fluctuations in the temporal dynamics of the acoustic subsystem by encoding the fluctuations into the topology of a complex network.

Two different sets of experiments were performed in a turbulent combustor with two different flame holding devices – bluff-body and vane swirler. The Reynolds number (Re) of the inlet airflow in the combustor was varied quasi-statically from $38,650 \pm 510$ to $67,590 \pm 720$ and $14,410 \pm 202$ to $27,520 \pm 320$, when bluff-body and vane swirler were used to stabilize the flame, respectively (details in Materials and Methods section). Fig. 1A shows the experimental setup. As we increase Re , the system exhibits a transition from a state of low-amplitude chaotic

fluctuations (Fig. 1D) to a state of high-amplitude stable limit cycle oscillations (Fig. 1F) via the route of intermittency (Fig. 1E).

We construct amplitude-transition networks (36,37) using normalized time series of acoustic pressure fluctuations (p'). The normalization is done with the maximum value of the acoustic pressure during the state of thermoacoustic instability. To construct the network, the data points of the time series are partitioned into discrete amplitude bins. Each amplitude bin corresponds to a node in the network. A directed link is established between two nodes if there is a transition between the corresponding amplitude bins in the time series of p' . The weight of the link is equal to the Markov transition probability between the two amplitude bins (details in the Materials and Methods section). Thus, the topology of the constructed network encodes the temporal order of fluctuations in the dynamics (41). Periodic oscillations would result in a regular network topology, where the connections exist between nodes that correspond to adjacent amplitude bins. On the other hand, chaotic fluctuations would be encoded as connections between nodes corresponding to non-adjacent amplitude bins and corresponding to different amplitude scales, and the network structure becomes more disorderly.

The Shannon entropy of the network (μ_S) (42) quantifies the network topology as defined by Eq. 1 (41, 43):

$$\mu_S = -\frac{\sum_j \sum_i w_{ij} \ln w_{ij}}{N} \quad (1)$$

Here, w_{ij} is the probability of the transition from node i to j , and N is the number of nodes in the network. For a complex network, the average network entropy quantifies the orderliness of connections between nodes and will be high when the network structure is more disorderly (41). We note that, for an amplitude transition network, the mean Shannon entropy (μ_S) quantifies the uncertainty in the transition between nodes corresponding to different amplitude scales owing

to fluctuations in the dynamics. Thus, μ_S is essentially a measure of chaotic intensity or chaotic content in the dynamics.

Also, Shannon entropy is equivalent to the Clausius entropy, which characterizes the macroscopic thermodynamic property of a system (44). Thus, μ_S of an amplitude-transition network encodes the uncertainty in temporal fluctuations of a dynamical system and also quantifies the thermodynamic disorder of the system.

Figure 2 shows the variation in μ_S of networks derived from acoustic pressure signal as the control parameter (Re) is varied quasi-statically in experiments. We find that μ_S varies non-monotonically with Re during the transition from chaos to order in both bluff-body (Fig. 2A) and swirl stabilized combustors (Fig. 2B). The value of μ_S increases up to a critical Reynolds number ($Re_c = 4.966 \times 10^4$ for bluff-body combustor and $Re_c = 1.724 \times 10^4$ for swirl combustor) and then decreases.

Such non-monotonic relation of a measure of disorder (μ_S) with the flow control parameter is compelling, as it implies that the thermodynamic disorder first increases and then decreases during the transition from chaos to order in the system. It is interesting that the temporal chaos gets stronger before the dynamics transitions to the state of intermittency (such as in Fig. 1E). Moreover, from Fig. 2C, we find that μ_S from both the combustors exhibit a similar power law scaling with p'_{rms} during both increase and decrease of chaotic content in the dynamics. Such scaling behavior is particularly useful as it allows us to understand the dynamical transition in the system even as the control parameter of the system changes.

The non-monotonous emergence of order reveals that during the transition from chaotic to periodic dynamics, there is an interplay between the mechanisms that promote order and disorder. A thermoacoustic system is a complex system where the acoustic, combustion, and hydrodynamic subsystems are nonlinearly coupled leading to synchronized co-evolution in these subsystems, thus promoting pattern formation and ordered dynamics. On the other hand, as we

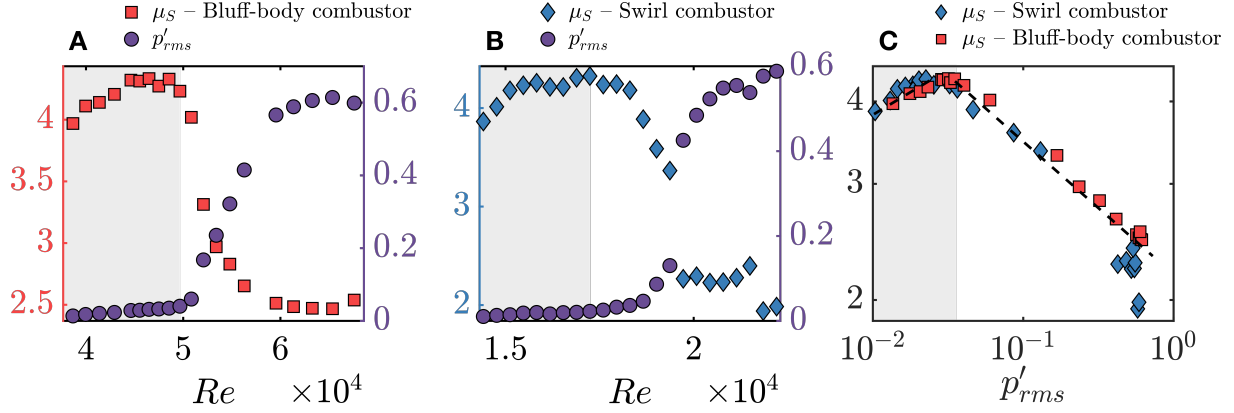


Figure 2: **The average Shannon entropy of transition networks, which quantifies the amount of disorder, first increases then decreases during the transition from chaos to order.** (A) Variation of average network entropy (μ_S) and root-mean-square of the non-dimensional pressure fluctuations p'_{rms} with the flow control parameter Re for a bluff-body stabilized turbulent combustor. The shaded region corresponds to the region where $Re < (Re_c)_{bluff}$ where $(Re_c)_{bluff} = 4.966 \times 10^4$. (B) Variation of average network entropy (μ_S) and root-mean-square of the pressure fluctuations (p'_{rms}) with the flow control parameter Re for a swirl stabilized turbulent combustor. The shaded region corresponds to the region where $Re < (Re_c)_{swirl}$ where $(Re_c)_{swirl} = 1.724 \times 10^4$. (C) μ_S from both bluff-body and swirl combustor exhibits a power law scaling $(\mu_S)_{bluff} \propto (p'_{rms})^\alpha$, and $(\mu_S)_{swirl} \propto (p'_{rms})^\beta$, respectively with similar exponents. The power law exponents for a bluff-body combustor when $Re < (Re_c)_{bluff}$ is $\alpha_1 = 0.09 \pm 0.024$, and when $Re > (Re_c)_{bluff}$ is $\alpha_2 = -0.19 \pm 0.009$. Similarly, the power law exponents for a swirl combustor when $Re < (Re_c)_{swirl}$ is $\beta_1 = 0.11 \pm 0.047$, and when $Re > (Re_c)_{swirl}$ is $\beta_2 = -0.23 \pm 0.032$.

increase the Reynolds number of the inlet flow, the turbulent intensity in the confined duct increases, promoting disorder. The non-monotonous emergence of order reveals that, during the transition from chaotic to periodic dynamics, disorder created by increasing turbulence intensity is dominant until a critical control parameter Re_c . Beyond this critical value Re_c , the nonlinear feedback dominates, causing disorder to decay monotonically. Moreover, the decrease in μ_S beyond the critical Reynolds number Re_c is a precursor for an impending thermoacoustic instability.

Further, we investigate the diversity in the magnitude of jumps between different amplitude scales associated with fluctuations. To do so, we use path-based centrality measures derived

from amplitude-transition networks. A path from one node to another in the network denotes the jump from one amplitude bin to another in the time series. Thus, we compute distance-based metrics such as characteristic path length (CPL) and mean betweenness centrality (\overline{C}_{BC}) to decipher the magnitude of jumps in amplitude due to fluctuations.

The CPL of a network is the mean number of steps needed to reach one node from another in the network (45, 46). For amplitude transition networks, CPL encodes the magnitude of jump in amplitude scale due to fluctuations between different amplitude bins (nodes). For example, in a periodic time series, any amplitude bin (node) is predominantly connected to its adjacent nodes. The difference in amplitude scales are small and of similar magnitude when transition occurs from any one bin to its neighboring bin, and this is reflected as a high value of CPL. On the other hand, a small value of CPL indicates that fluctuations occur between nodes of very different amplitude scales, such as during chaotic dynamics.

The betweenness centrality of a node quantifies the extent to which a node lies in the path between other nodes of the network (46, 47). For an amplitude transition network, the mean betweenness centrality \overline{C}_{BC} quantifies the order in which transition occurs between different amplitude scales. If there are direct transitions between bins of diverse amplitude scales, such as during chaotic fluctuations, then the value of \overline{C}_{BC} will be low. However, for a periodic time series, the connections are mostly between adjacent nodes, and any node lies ‘in between’ the path of many other node pairs with different amplitude scales, resulting in a high value for \overline{C}_{BC} .

The variation of CPL and \overline{C}_{BC} with p'_{rms} derived from a bluff-body and swirl-stabilized turbulent combustor is shown in Fig. 3A and Fig. 3B, respectively. Clearly, both the measures are minimum during chaotic dynamics and reach a maximum during periodic dynamics (thermoacoustic instability). We infer that the variation in the magnitudes of jumps in amplitude scales due to fluctuations decrease in a monotonic fashion as order emerges amidst chaos in the system. Note that, as Re increases in the regime $Re < Re_c$, fluctuations become more random

and uncertain, and the chaotic content increases (μ_S increases), while the amplitude scales associated with the fluctuations become less diverse (CPL and \overline{C}_{BC} increase). For $Re > Re_c$, both the chaotic intensity and the range of amplitude scales in which the fluctuations occur decrease (μ_S decreases, CPL and \overline{C}_{BC} increase). Moreover, CPL and \overline{C}_{BC} exhibit distinct power law scaling behavior with the root-mean-square of acoustic pressure fluctuations. The power law exponents are nearly identical for experiments in both bluff-body and swirl stabilized turbulent combustor.

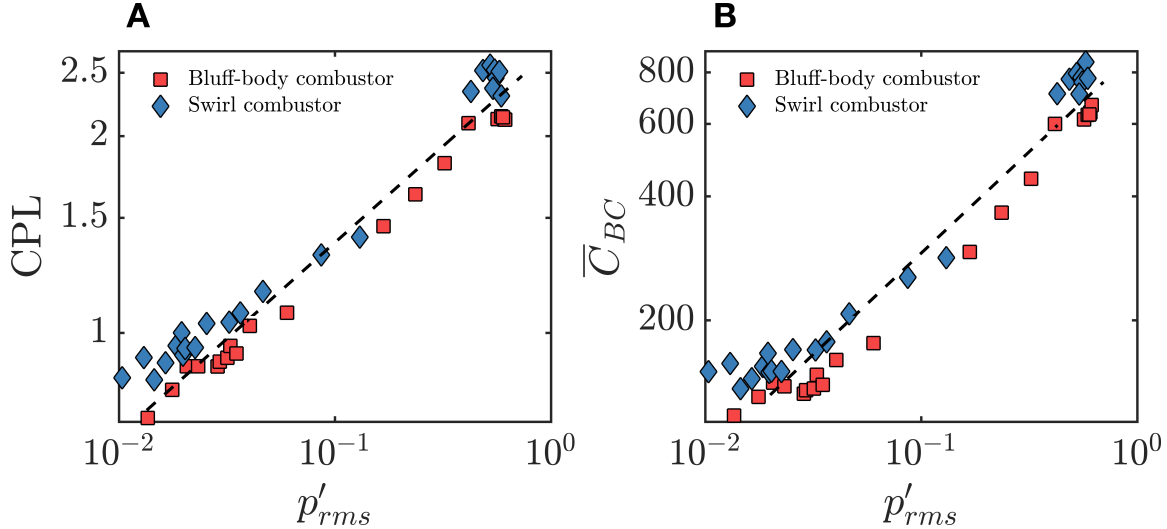


Figure 3: Quantifying diversity in amplitude scale of fluctuations using distance-based network topological metrics. (A) Variation of characteristic path length (CPL) of network constructed from time series of non-dimensional p' of bluff-body and swirl stabilized turbulent combustor with p'_{rms} . The measure from both combustors exhibits the same power law scaling $CPL \propto (p'_{rms})^\gamma$, with exponent $\gamma = 0.28 \pm 0.016$. (B) Variation of average betweenness centrality (\overline{C}_{BC}) of network constructed from time series of non-dimensional p' of bluff-body and swirl stabilized turbulent combustor with p'_{rms} . \overline{C}_{BC} from the bluff-body and swirl combustor exhibits a similar power law scaling $\overline{C}_{BC} \propto (p'_{rms})^\kappa$ with exponents $\kappa = 0.48 \pm 0.033$ and $\kappa = 0.47 \pm 0.036$, respectively.

In summary, we used complex networks to characterize the fluctuations and the jumps in amplitudes due to fluctuations as a dynamical transition occurs in a complex turbulent thermo-fluid system. Intriguingly, during the transition from chaos to order, we discover a regime

where the amount of uncertainty in fluctuations increases, but the amplitude jumps become less diverse.

DISCUSSION

Several complex systems exhibit self-organization owing to an ensemble of elements that interact nonlinearly with each other. The nonlinear interactions between sub-units of a complex system can lead to continuous or abrupt emergence of self-sustained ordered dynamics. For example, a continuous transition to ordered dynamics occurs in a system of chemical oscillators (38), whereas order emerges abruptly in the magnetic properties of ferromagnetic materials (40). Here, we discover that order emerges non-monotonically in a turbulent reacting flow confined in a duct coupled to the acoustic field of the duct.

We use a complex networks approach to encode the fluctuations in the system dynamics and use network measures to quantify the characteristics of fluctuations during the transition from chaos to order in the system. The network is constructed by binning amplitudes and encoding the transition probabilities due to fluctuations between these bins, and is referred to as amplitude transition networks. The mean entropy μ_S of an amplitude transition network captures the uncertainty in the amount of fluctuations between different amplitude scales and reflects the chaotic intensity of the dynamics. On the other hand, distance-based network metrics (CPL and \overline{C}_{BC}) indicate the diversity in the jumps in amplitude scales due to fluctuations in the time series. Thus, our approach offers a novel means to understand as well as quantify the emergence of order through fluctuations, as proposed by Prigogine (18). This approach explicitly investigates how fluctuations evolve and if the amplitude scales diversify during a dynamical transition.

We find that, during the transition from chaos to order in a complex turbulent thermo-fluid system, μ_S first increases and then decreases, whereas CPL and \overline{C}_{BC} increase monotonically.

Thus, the chaotic intensity of fluctuations decreases non-monotonically, whereas the diversity of magnitude of amplitude jumps decreases monotonically during the emergence of order from chaos in an acoustically-coupled turbulent thermo-fluid system.

Moreover, we observed that the scaling behavior for all the measures are similar for two different experimental operating conditions using distinct flame holding devices in a turbulent combustor. Our findings imply that the underlying turbulence and the nonlinear feedback between subsystems compete to dominate the dynamics of the system. We are able to identify the critical value Re_c , where the inter-subsystem interactions begin to dominate the influence of the underlying turbulence, allowing self-sustained ordered dynamics to emerge in the flow.

Our approach using complex networks to encode the fluctuations is novel and can be extended to study dynamical transitions in several systems. By encoding the fluctuations as the topology of a network, we also encode the structure of interactions in the system that influence these fluctuations. Additionally, we propose that using measures derived from amplitude transition networks, one can quantify as well as compare the different types of dynamical transitions across systems, such as monotonic, non-monotonic, or abrupt transition between chaos and order.

MATERIALS AND METHOD

EXPERIMENTAL SETUP

We conducted experiments in a bluff-body stabilized and swirl-stabilized turbulent combustor. A schematic of the turbulent combustor used in this study is shown in Fig. 1. The turbulent combustor comprises a plenum chamber, a burner, and a combustion chamber with ducts. Another chamber with a relatively larger cross-sectional area, known as the decoupler, is connected to one end of the combustion duct. The decoupler ensures that the pressure at the end of the duct is equal to the ambient pressure, making the fluctuations at the boundary insignificant. A central

shaft of diameter 16 mm through the burner supports the flame-stabilizing circular disc object, i.e., a bluff-body (Fig. 1B) or a vane swirler (Fig. 1C).

Compressed air enters the plenum chamber of the combustor before passing through the burner, where the mixing of the air and fuel (liquefied petroleum gas) takes place. The central shaft delivers fuel into the combustion chamber via four radial injection holes with diameters of 1.7 mm each. The dynamics of the unsteady acoustic pressure oscillations in the combustor is investigated as the system parameter, i.e., the Reynolds number of the incoming flow is varied. The acoustic pressure fluctuations in the combustion chamber are acquired using a piezoelectric pressure transducer (PCB103B02, with an uncertainty of ± 0.15 Pa). The transducer is mounted at a distance of 25 mm from the dump plane and records the pressure signal for 3 s at a sampling rate of 10 kHz.

The Reynolds number near the position of the burner is calculated as $Re = 4\dot{m}D_1/\pi\mu D_0^2$, where \dot{m} is the sum of air-flow rate (\dot{m}_a) and fuel-flow rate (\dot{m}_f), D_0 is the hydraulic diameter of the burner, D_1 is the diameter of the circular bluff-body ($D_1 = D_0$ for experiments with swirler) and μ is the kinematic viscosity of the fuel-air mixture at the experimental condition. We use the expression for dynamic viscosity as stated by Wilke (48) to compute the Reynolds number of a binary gas mixture.

For experiments on a bluff-body stabilized turbulent combustor, the fuel flow is set constant at 48 SLPM (standard liter per minute), and the airflow is varied from 752 – 1446 SLPM quasi-statically (i.e., the Reynolds number is varied from $(3.865 \pm 0.051) \times 10^4$ to $(6.759 \pm 0.072) \times 10^4$). Similarly, for the experiments on a swirl-stabilized turbulent combustor, we set a constant fuel flow rate of 21 SLPM, and the airflow rate is varied from 330 – 550 SLPM quasi-statically (i.e., the Reynolds number is varied from $(1.441 \pm 0.020) \times 10^4$ to $(2.752 \pm 0.032) \times 10^4$).

CONSTRUCTION OF AMPLITUDE TRANSITION NETWORKS

We use the stochastic mapping network construction technique proposed by Shiraziet *al.* (36), which explicitly encodes the temporal sequence of the considered variable. For a discrete time series $x(t) = \{x_1, x_2, \dots, x_n\}$, we begin the network construction by grouping these data points into horizontal amplitude-bins, i.e., discrete ‘states.’ The number of bins required and the respective width of each bin are chosen such that the number of data points in each bin is approximately equal. The number of bins (N) needed for this formulation is given by $N \approx 2n^{2/5}$ as obtained via chi-square goodness-of-fit test (49).

Each bin is considered a node in the network. There exists a link between node i and j if the variable $x(t)$ changes from i^{th} bin to j^{th} bin in one-time step. We define a matrix $\mathbf{A} = a_{ij}$, where a_{ij} is the total number of transitions of the variable $x(t)$ from bin i to j . We then compute the transitional probability matrix $\mathbf{W} = w_{ij}$, where w_{ij} is the probability of a Markov chain transition from node (bin) i to j and is given by $p[x(t) | x(t - 1)]$, i.e., $w_{ij} = a_{ij} / \sum_j a_{ij}$. We attribute w_{ij} as the weight to the link from node i to node j in the network. Thus, \mathbf{W} is the adjacency matrix for the network.

High-frequency fluctuations due to noise or turbulence reflect as small variations in the amplitude of p' . We can average out such variations by modifying the timescale over which we compute transitions between bins. To do so, the transition matrix is constructed with elements of the matrix w_{ij} given by $p[x(t) | x(t - \tau)]$, where τ is the transition timescale. Figure 4(A,C) shows the network constructed from a noisy signal with $\tau = 3$. Figure 4B shows a schematic series where we use $\tau = 3$ while counting transitions. The weight $w_{ij} = p[x(t) | x(t - 3)]$, i.e., we consider the transition between A_1 and A_2 , B_1 and B_2 , C_1 and C_2 (Fig. 4B) and so on to find the number of transition from one bin to another. To find an optimal transition timescale (τ_{opt}), we compute the average network entropy (μ_S) for the network constructed from the acoustic pressure signal obtained during the dominant acoustic mode for different values of τ . Then, τ_{opt}

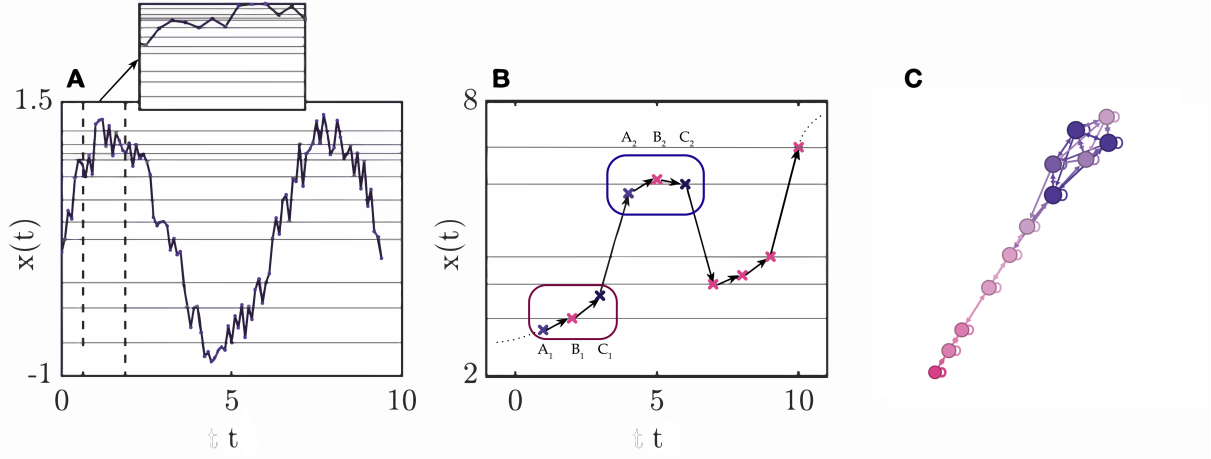


Figure 4: **Schematic for network construction.** (A) A noisy sinusoidal signal, $x(t) = \sin(x) + \xi$, where ξ represents uniformly distributed random noise. There are 95 data points cumulatively partitioned into 12 bins, each containing approximately 8 data points. (B) Representative figure to examine the network formation for a transition timescale of $\tau = 3$. (C) A stochastic mapping network constructed from the noisy sine signal. The constructed network is visualized with Force-Atlas algorithm (50) in the software Gephi (51).

is chosen as the value of τ for which μ_S is maximum. We obtain $\tau_{opt} = 20$ for both bluff-body (Fig. 5) and swirl combustor.

To facilitate comparison across different dynamical states, we ensure a common set of nodes (amplitude bins) for all the time series p' obtained when Re in the bluff-body combustor is varied in a quasi-static manner between $(3.865 \pm 0.051) \times 10^4$ and $(6.759 \pm 0.072) \times 10^4$ ($(1.441 \pm 0.020) \times 10^4$ to $(2.752 \pm 0.032) \times 10^4$) for a swirl combustor). The total number of bins obtained is $N = 418$ (bluff-body combustor) and $N = 433$ (swirl combustor). For each quasi-static experiment, we construct a transition network by calculating the transition probabilities between nodes for the corresponding time series of p' obtained from the experiments.

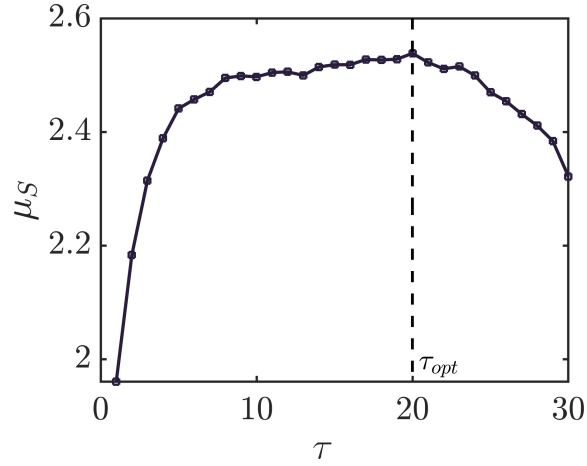


Figure 5: **Finding the optimal transition timescale τ .** Variation of average network entropy μ_S corresponding to the time series of p' corresponding to thermoacoustic instability ($Re = 6.759 \times 10^4$) and τ . Here, $\tau_{opt} = 20$.

Acknowledgements: The authors thank S. Sivakumar, Anaswara Bhaskaran, P. R. Midhun, S. Thilagaraj, S. Anand (Indian Institute of Technology, Madras) and Dr. Samadhan A. Pawar (University of Toronto) for providing the experimental data.

Funding: We acknowledge the funding for this work from J. C. Bose Fellowship (No. JCB/2018/000034/SSC) and the IoE initiative (SB/2021/0845/AE/MHRD/002696). ST also acknowledges the support from Prime Minister Research Fellowship, Govt. of India.

Author contributions: Conceptualization: ST, RIS. Methodology and analysis: AB, ST. Interpretation: AB, ST, NM, JK, RIS. Visualization: AB. Supervision: NM, JK, RIS. Writing—original draft: AB, ST. Writing—review & editing: AB, ST, NM, JK, RIS.

Competing interests: The authors declare no competing interests.

Data and materials availability: The data used in this study are available from the corresponding author upon reasonable request.

References

1. J. Buck, E. Buck, Synchronous fireflies. *Sci. Am.* **234**, 74–85 (1976).
2. Z. Néda, E. Ravasz, Y. Brechet, T. Vicsek, A.-L. Barabási, The sound of many hands clapping. *Nature* **403**, 849–850 (2000).
3. E. B. Bromfield, J. E. Cavazos, J. I. Sirven, *An Introduction to Epilepsy* (American Epilepsy Society, 2006).
4. I. R. Epstein, J. A. Pojman, *An Introduction to Nonlinear Chemical Dynamics: Oscillations, Waves, Patterns, and Chaos* (Oxford Univ. Press, 1998).
5. S. Jakubith, H.-H. Rotermund, W. Engel, A. Von Oertzen, G. Ertl, Spatiotemporal concentration patterns in a surface reaction: Propagating and standing waves, rotating spirals, and turbulence. *Phys. Rev. Lett.* **65**, 3013 (1990).
6. W. Friesen, G. Block, What is a biological oscillator? *Am. J. Physiol. Regul. Integr. Comp. Physiol.* **246**, R847–R853 (1984).
7. P. Bergé, M. Dubois, Rayleigh-bénard convection. *Contemp. Phys.* **25**, 535–582 (1984).
8. R. A. Oliva, S. H. Strogatz, Dynamics of a large array of globally coupled lasers with distributed frequencies. *Int. J. Bifurcat. Chaos* **11**, 2359–2374 (2001).
9. H. Gotoda, Y. Shinoda, M. Kobayashi, Y. Okuno, S. Tachibana, Detection and control of combustion instability based on the concept of dynamical system theory. *Phys. Rev. E* **89**, 022910 (2014).
10. V. Nair, R. I. Sujith, Precursors to self-sustained oscillations in aeroacoustic systems. *Int. J. Aeroacoust.* **15**, 312–323 (2016).

11. H. Gotoda, H. Kinugawa, R. Tsujimoto, S. Domen, Y. Okuno, Characterization of combustion dynamics, detection, and prevention of an unstable combustion state based on a complex-network theory. *Phys. Rev. Appl.* **7**, 044027 (2017).
12. R. I. Sujith, V. R. Unni, Complex system approach to investigate and mitigate thermoacoustic instability in turbulent combustors. *Phys. Fluids* **32**, 061401 (2020).
13. R. I. Sujith, S. A. Pawar, *Thermoacoustic Instability* (Springer International Publishing, 2021).
14. A. Jenkins, Self-oscillation. *Phys. Rep.* **525**, 167–222 (2013).
15. J. Venkatramani, V. Nair, R. I. Sujith, S. Gupta, S. Sarkar, Precursors to flutter instability by an intermittency route: a model free approach. *J. Fluids Struct.* **61**, 376–391 (2016).
16. L. v. Bertalanffy, *General System Theory: Foundations, Development, Applications* (G. Braziller, 1968).
17. S. A. Kauffman, *At Home in the Universe: The Search for Laws of Self-Organization and Complexity* (Oxford Univ. Press, USA, 1995).
18. I. Prigogine, Time, structure, and fluctuations. *Science* **201**, 777–785 (1978).
19. B.-T. Chu, L. S. G. Kovásznyai, Non-linear interactions in a viscous heat-conducting compressible gas. *J. Fluid Mech.* **3**, 494–514 (1958).
20. T. C. Lieuwen, V. Yang, *Combustion Instabilities in Gas Turbine Engines: Operational Experience, Fundamental Mechanisms, and Modeling* (AIAA, 2005).
21. S. Tandon, R. I. Sujith, Multilayer network analysis to study complex inter-subsystem interactions in a turbulent thermoacoustic system. *J. Fluid Mech.* **966**, A9 (2023).

22. M. Avila, D. Barkley, B. Hof, Transition to turbulence in pipe flow. *Annu. Rev. Fluid Mech.* **55** (2022).
23. C. V. Tran, The number of degrees of freedom of three-dimensional Navier–Stokes turbulence. *Phys. Fluids* **21**, 125103 (2009).
24. N. B. George, V. R. Unni, M. Raghunathan, R. I. Sujith, Pattern formation during transition from combustion noise to thermoacoustic instability via intermittency. *J. Fluid Mech.* **849**, 615–644 (2018).
25. J. Tony, E. A. Gopalakrishnan, E. Sreelekha, R. I. Sujith, Detecting deterministic nature of pressure measurements from a turbulent combustor. *Phys. Rev. E* **92**, 062902 (2015).
26. V. Nair, G. Thampi, R. I. Sujith, Intermittency route to thermoacoustic instability in turbulent combustors. *J. Fluid Mech.* **756**, 470–487 (2014).
27. S. A. Pawar, A. Seshadri, V. R. Unni, R. I. Sujith, Thermoacoustic instability as mutual synchronization between the acoustic field of the confinement and turbulent reactive flow. *J. Fluid Mech.* **827**, 664–693 (2017).
28. Y. Okuno, M. Small, H. Gotoda, Dynamics of self-excited thermoacoustic instability in a combustion system: Pseudo-periodic and high-dimensional nature. *Chaos* **25**, 043107 (2015).
29. M. Murugesan, R. I. Sujith, Combustion noise is scale-free: transition from scale-free to order at the onset of thermoacoustic instability. *J. Fluid Mech.* **772**, 225–245 (2015).
30. V. Godavarthi, V. Unni, E. Gopalakrishnan, R. I. Sujith, Recurrence networks to study dynamical transitions in a turbulent combustor. *Chaos* **27**, 063113 (2017).

31. H. Gotoda, H. Kinugawa, R. Tsujimoto, S. Domen, Y. Okuno, Characterization of combustion dynamics, detection, and prevention of an unstable combustion state based on a complex-network theory. *Phys. Rev. Appl.* **7**, 044027 (2017).
32. V. Godavarthi, S. A. Pawar, V. R. Unni, R. I. Sujith, N. Marwan, J. Kurths, Coupled interaction between unsteady flame dynamics and acoustic field in a turbulent combustor. *Chaos* **28**, 113111 (2018).
33. T. Kobayashi, S. Murayama, T. Hachijo, H. Gotoda, Early detection of thermoacoustic combustion instability using a methodology combining complex networks and machine learning. *Phys. Rev. Appl.* **11**, 064034 (2019).
34. T. Hashimoto, H. Shibuya, H. Gotoda, Y. Ohmichi, S. Matsuyama, Spatiotemporal dynamics and early detection of thermoacoustic combustion instability in a model rocket combustor. *Phys. Rev. E* **99**, 032208 (2019).
35. S. Tandon, R. I. Sujith, Condensation in the phase space and network topology during transition from chaos to order in turbulent thermoacoustic systems. *Chaos* **31**, 043126 (2021).
36. A. Shirazi, G. R. Jafari, J. Davoudi, J. Peinke, M. R. R. Tabar, M. Sahimi, Mapping stochastic processes onto complex networks. *J. Stat. Mech. Theory Exp.* **2009**, P07046 (2009).
37. Q. Yuan, J. Zhang, H. Wang, C. Gu, H. Yang, A multi-scale transition matrix approach to chaotic time series. *Chaos Solit. Fractals.* **172**, 113589 (2023).
38. I. Z. Kiss, Y. Zhai, J. L. Hudson, Emerging coherence in a population of chemical oscillators. *Science* **296**, 1676–1678 (2002).

39. A. Chatterjee, N. Mears, Y. Yadati, G. S. Iannacchione, An overview of emergent order in far-from-equilibrium driven systems: From Kuramoto oscillators to Rayleigh–Bénard convection. *Entropy* **22** (2020).
40. J. Kouvel, C. Hartelius, Abrupt magnetic transition in MnSn_2 . *Phys. Rev.* **123**, 124 (1961).
41. M. Wiedermann, J. F. Donges, J. Kurths, R. V. Donner, Mapping and discrimination of networks in the complexity-entropy plane. *Phys. Rev. E* **96**, 042304 (2017).
42. C. E. Shannon, A mathematical theory of communication. *The Bell system technical journal* **27**, 379–423 (1948).
43. M. Small, *2013 IEEE International Symposium on Circuits and Systems (ISCAS)* (IEEE, 2013), pp. 2509–2512.
44. M. Weilenmann, L. Kraemer, P. Faist, R. Renner, Axiomatic relation between thermodynamic and information-theoretic entropies. *Phys. Rev. Lett.* **117**, 260601 (2016).
45. R. Albert, A.-L. Barabási, Statistical mechanics of complex networks. *Rev. Mod. Phys.* **74**, 47–97 (2002).
46. M. Rubinov, O. Sporns, Complex network measures of brain connectivity: Uses and interpretations. *NeuroImage* **52**, 1059–1069 (2010). *Computational Models of the Brain*.
47. L. C. Freeman, A set of measures of centrality based on betweenness. *Sociometry* pp. 35–41 (1977).
48. C. Wilke, A viscosity equation for gas mixtures. *J. Chem. Phys.* **18**, 517–519 (1950).
49. W. F. Guthrie, NIST/SEMATECH e-handbook of Statistical Methods (NIST handbook 151) (2020).

50. M. Jacomy, T. Venturini, S. Heymann, M. Bastian, Forceatlas2, a continuous graph layout algorithm for handy network visualization designed for the gephi software. *PLoS One* **9**, e98679 (2014).
51. M. Bastian, S. Heymann, M. Jacomy, Gephi: An open source software for exploring and manipulating networks. *Proceedings of the International AAAI Conference on Web and Social Media* **3**, 361-362 (2009).